

# Heat transfer enhancement in internally finned tubes accounting for combined convection and participating radiation

JUAN C. MORALES

Departamento de Mecánica, Universidad Simón Bolívar, Caracas 1080-A, Venezuela

ANTONIO CAMPO

Miami, FL 33172, U.S.A.

and

CARLOS SCHULER

Department of Mechanical Engineering, University of California, Berkeley, CA 94720, U.S.A.

(Received 9 March 1990 and in final form 19 September 1990)

**Abstract**—This paper presents an analysis of the simultaneous heat transfer by forced convection, radiation and conduction in the entrance region of an internally finned circular tube. The governing equations of momentum, energy and radiative transfer are solved numerically using a control volume based approach. Under the idealization of a gray gas, the radiative contribution in the medium is modeled by an approximate differential method, the first-order spherical harmonics ( $P_1$ ) approximation. This route provides an additional partial differential equation of elliptic type in the system of convection-diffusion equations. Adoption of this differential formulation is advantageous from a computational point of view, because it is fully compatible with the SIMPLER code. Computed results for the distorted velocity profiles in the reduced cross-section of the tube provide the frictional losses due to the addition of longitudinal fins. Furthermore, heat transfer augmentation in the thermal entrance region of the finned tube is represented by the mean bulk temperature in terms of the descriptive geometric, hydrodynamic, thermal and radiative parameters.

## INTRODUCTION

THE AUGMENTATION of the heat transfer performance of circular tubes by longitudinal internal fins has found wide use in compact heat exchangers due to the additional surface area provided by the fins. In this regard, an extensive review of heat transfer enhancement techniques has been presented by Bergles [1], wherein various internal fin arrangements are described in detail.

Previous theoretical and experimental investigations of laminar flow and heat transfer in internally finned tubes have dealt almost exclusively with the hydrodynamically and thermally developed situation. In these studies, the thermal conductivity of the tube wall and the longitudinal fins has been assumed to be sufficiently high so that the fins remain at a uniform temperature approximately. Furthermore, in these studies the fin thickness in the array has been usually considered negligible in comparison with the interfin spacing. Accordingly, the corresponding numerical results have been reported in terms of two asymptotic parameters: the friction factor and the fully developed Nusselt number, both expressed as a function of the fin height and the number of fins in the array.

More recently, it has been realized by different researchers that the complex interaction of fluid flow and heat transfer in internally finned tubes of compact heat exchangers necessitates to produce additional calculations in the developing region. Obviously, this was necessary in order to complement the information already available for the fully developed region. In view of this limitation, Rustum and Soliman [2] conducted a numerical analysis of the fully developed laminar flow and developing temperature in longitudinally finned tubes. These authors used standard finite-difference procedures for their calculations. On the other hand, Prakash and Liu [3] and Choudhary and Patankar [4] examined the situation of simultaneously developing fluid flow and heat transfer in a tube with longitudinally internal fins. In these two independent publications [3, 4], the applicable conservation equations were solved numerically utilizing a control volume based discretization in conjunction with the SIMPLER code.

Conversely, heat transfer by simultaneous convective and radiative transfer in gas flows operating at high temperature and high heat fluxes has become increasingly important in the area of high temperature heat exchangers. The available results have been sum-

## NOMENCLATURE

$A_f$	dimensionless flow area	$T$	absolute temperature [K]
$c_p$	specific heat at constant pressure [J kg <sup>-1</sup> K <sup>-1</sup> ]	$T_{ref}$	reference temperature, $T_{ref} = T_w$ [K]
$f$	friction factor, equation (7)	$T_b$	mean bulk temperature [K]
$G$	total irradiation [W m <sup>-2</sup> ]	$T_c$	entrance temperature [K]
$G^*$	dimensionless total irradiation, equation (6)	$T_w$	wall temperature [K]
$H$	dimensionless fin height, $h/r_0$	$t$	dimensionless temperature, equation (6)
$h$	fin height [m]	$U$	dimensionless velocity, equation (6)
$I$	intensity of radiation [W m <sup>-2</sup> sr <sup>-1</sup> ]	$\bar{U}$	dimensionless mean velocity
$I_b$	intensity of black body radiation [W m <sup>-2</sup> sr <sup>-1</sup> ]	$u$	velocity [m s <sup>-1</sup> ]
$K_a$	total volumetric absorption coefficient [m <sup>-1</sup> ]	$\bar{u}$	mean velocity [m s <sup>-1</sup> ]
$k$	thermal conductivity [W m <sup>-1</sup> K <sup>-1</sup> ]	$Z$	dimensionless axial coordinate, equation (6)
$\dot{m}$	mass flow rate [kg s <sup>-1</sup> ]	$Z^+$	dimensionless axial coordinate, equation (14)
$N$	radiation-conduction parameter, equation (6)	$z$	axial coordinate [m].
$NF$	number of fins	Greek symbols	
$Pr$	Prandtl number	$\alpha$	half the angle between the sides of adjacent fins
$p$	pressure [N m <sup>-2</sup> ]	$\beta$	half the angle subtended by one fin
$\mathbf{p}$	position vector [m]	$\hat{\beta}$	extinction coefficient [m <sup>-1</sup> ]
$Q_T$	total heat transfer, equation (10) [W]	$\eta$	dimensionless radial coordinate, equation (6)
$Q_x$	ideal heat transfer [W]	$\theta$	angular coordinate
$\mathbf{q}^R$	radiation flux vector [W m <sup>-2</sup> ]	$\nu$	kinematic viscosity [m <sup>2</sup> s <sup>-1</sup> ]
$Re$	Reynolds number for finned tube, equation (6)	$\rho$	density [kg m <sup>-3</sup> ]
$Re_s$	Reynolds number for smooth tube, equation (14)	$\sigma$	Stefan-Boltzmann constant [W m <sup>-2</sup> K <sup>-4</sup> ]
$r$	radial coordinate [m]	$\tau$	optical thickness, equation (6)
$r_0$	pipe radius [m]	$\omega$	solid angle
		$\Omega$	heat transfer efficiency, equation (12).

marized and discussed recently by Howell [5] in a review paper and by Mori *et al.* [6] in a monograph. In these applications, unless the contribution of radiation is very weak or very strong, momentum, energy and radiative transport equations must be solved simultaneously in order to determine local temperatures and local heat fluxes in the participating gas medium. The rigorous formulation of the energy equation describing laminar forced convection of a gas that emits and absorbs radiation in a plain tube involves a non-linear integro-partial differential equation [5]. In fact, it is also well known that the numerical solution of this intricate equation is quite involved and requires large amounts of computing time and storage. In this regard, in order to carry out the computations it is usually necessary to implement an iterative approach in which the integral terms and the differential terms of the above-cited energy equation are solved consecutively [7-9]. Alternatively, the approximate differential methods documented by Ozisik [10] seek to replace the highly complex energy equation and the radiative transfer equation (RTE) by a system of coupled partial differential equations

that depend on both temperature and irradiation. As a result, the numerical solution of this transformed system seems to be easier to obtain than the original integro-partial differential equation. In this sense, the first moment method and the  $P_1$ -approximation of the spherical harmonics are equivalent procedures that accomplish this goal [10]. At this stage, it should be mentioned that this particular methodology has been successfully employed in ref. [11] for the investigation of a thermally developing radiative-convective gas flow restricted to fully developed velocity. The numerical solution of the transformed system of ordinary differential equations of first order was readily obtained in ref. [11] via a novel combination of the method of lines, control volume discretization and a Runge-Kutta algorithm.

Although a number of analyses dealing with combined problems of forced convection and radiative transfer have been performed under the assumption that a fully developed temperature prevails, this idealization may provide erroneous thermal results. In this respect, two publications one by Kurosaki [12] and the other by Chawla and Chan [13] have tacitly dem-

onstrated that the axial variation of the total Nusselt number possesses a concave shape (passing through a minimum), rather than gradually approach an asymptotic value characteristic of pure forced convection tube flows.

In light of the foregoing, the primary objective of this paper is to explore the combined enhancing effects of participating thermal radiation on laminar forced convection of gas flows through internally longitudinal finned tubes. An exhaustive literature review on the subject of combined mechanisms of heat transmission reflects that this kind of problem has not been investigated so far. However, the question of forced convection in laminar duct flows under the influence of surface radiative exchange has been addressed recently by Torikoshi *et al.* [14] and Chan and Kumar [15]. For concreteness, the present analysis focused on a general situation wherein the gas temperature develops in a longitudinal finned tube, and the velocity is taken as fully developed. The computed velocity, of course, depends on the fin height and the specific number of fins deployed in the tube cross-section. Hence, this distorted velocity profile is considered as an input for the governing equation of energy conservation.

Turning attention to the radiative analysis, as a first-order approximation, the medium is assumed as a gray gas, capable of emitting and absorbing radiant energy. Furthermore, the inner tube surface is considered black, whereas the fins are relatively thick and are equally distributed in the cross-section of the tube. The applicable RTE, based on the  $P_1$ -approximation is coupled with the SIMPLER code which is used to solve the set of conservation equations numerically. Computed results are presented at the end of the paper for the axial variation of the mean bulk temperatures as a function of the controlling parameters describing the combined heat exchange process. These results will be useful to the design engineer for predicting the level of heat transfer augmentation (due to the action of combined mechanisms and a fixed number of fins) in the thermal entrance region of the tube. In addition to this, the results also provide parallel hydrodynamic data associated to the increase of pressure losses due to finning.

## DIFFERENTIAL FORMULATION

The analysis is referred to the cross-section of the internally finned tube shown in Fig. 1. By virtue of the symmetries, it is only necessary to analyze the flow and heat transfer processes in the sector that spans between the tube centerline,  $\theta = 0^\circ$ , the tube wall, and the angle  $\theta = \alpha + \beta$ . In other words, the integration domain corresponds to a sector constructed between any two consecutive fins and the wall. Furthermore, the tube wall and the array of straight fins were supposed to be of high thermal conductivity, so that both would assume a uniform temperature over the cross-section of the tube.

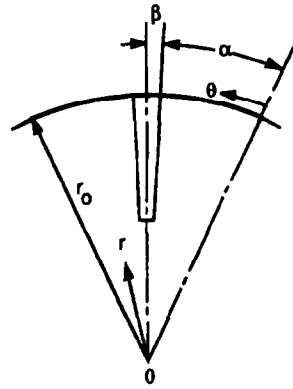


FIG. 1. Cross-section of the internally finned tube.

For the situation of fully developed laminar flow in the finned tube, the equations of conservation for a radiatively participating gas may be written as follows:

momentum

$$\frac{1}{\eta} \frac{\partial}{\partial \eta} \left( \eta \frac{\partial U}{\partial \eta} \right) + \frac{1}{\eta^2} \frac{\partial^2 U}{\partial \theta^2} + 1 = 0; \quad (1)$$

energy

$$\frac{1}{2} \frac{U}{\bar{U}} \frac{\partial t}{\partial z} = \frac{1}{\eta} \frac{\partial}{\partial \eta} \left( \eta \frac{\partial t}{\partial \eta} \right) + 4N\tau(G^* - t^4) + \frac{1}{\eta^2} \frac{\partial^2 t}{\partial \theta^2}; \quad (2)$$

radiative transfer

$$\frac{1}{\eta} \frac{\partial}{\partial \eta} \left( \eta \frac{\partial G^*}{\partial \eta} \right) + \frac{1}{\eta^2} \frac{\partial^2 G^*}{\partial \theta^2} = 3\tau^2(G^* - t^4) \quad (3)$$

where the step-by-step derivation of equations (2) and (3) is given in the Appendix.

To complete the formulation of the foregoing problem, the hydrodynamic boundary conditions applied to equation (1) are:  $U = 1$  at the entrance,  $U = 0$  on the solid walls,  $\partial U / \partial \theta = 0$  on the symmetry lines, and  $\partial U / \partial \eta = 0$  at the centerline of the tube. The thermal boundary conditions imposed on equation (2) are:  $t = t_e$  at the entrance,  $t = 1$  at the solid walls ( $T_{\text{ref}} = T_w$ ),  $\partial t / \partial \theta = 0$  on the symmetry lines, and  $\partial t / \partial \eta = 0$  at the centerline of the tube. Moreover, equation (3) was solved subject to the boundary conditions controlling the dimensionless irradiation  $G^*$  at the solid black walls (including the array of fins), namely

$$\frac{\partial G^*}{\partial n} = -\frac{3}{2}\tau(G^* - t^4) \quad \text{at the solid walls} \quad (4)$$

$$\frac{\partial G^*}{\partial n} = 0 \quad \text{on the symmetry lines} \quad (5)$$

where  $\partial / \partial n$  designates the normal derivative.

The preceding set of equations has been formulated with the following dimensionless variables and descriptive parameters:

$$\begin{aligned}
 U &= \frac{u}{r_0^2(-dp/dz)/\mu}, \quad \eta = \frac{r}{r_0}, \quad t = \frac{T}{T_{\text{ref}}} \\
 Z &= \frac{z}{r_0 Re Pr}, \quad Re = \frac{2\bar{u}r_0}{\nu}, \quad \tau = \beta r_0 \\
 G^* &= \frac{G}{4\sigma T_{\text{ref}}^4}, \quad N = \frac{\sigma r_0 T_{\text{ref}}^3}{k}
 \end{aligned} \quad (6)$$

where the symbols are defined in the Nomenclature. Additionally, the foregoing formulation is restricted to uniform fluid properties, where the influence of viscous dissipation, axial conduction and axial radiation in the gas domain have been considered negligible.

### HYDRODYNAMIC AND THERMAL PARAMETERS

The hydrodynamic aspects of the combined problem defined in the preceding section will be analyzed first. Hence, according to Soliman and Feingold [16], the pressure drop due to internal finning, may be conveniently presented through the value of  $f Re$

$$f Re = \frac{2\pi/A_f}{\bar{U}} \quad (7)$$

where  $A_f$  is the dimensionless flow area given by the relation

$$A_f = \pi - (NF)\beta(2-H)H. \quad (8)$$

Correspondingly, this same approach was used in the present paper for correlating the computed friction factor of internally finned tubes. In addition, it also serves to provide a basis of comparison with smooth (finless) tubes, retaining the same numerical values of the tube radius  $r_0$ , the kinematic viscosity of the fluid  $\nu$  and the mass flow rate  $\dot{m}$ .

Secondly, for the heat transfer calculations, the thermal quantity of paramount interest is the mean bulk temperature distribution, which is defined as

$$t_b = \frac{\int_{A_f} U t \, dA_f}{\int_{A_f} U \, dA_f} \quad (9)$$

where the integration was performed over the dimensionless flow area  $A_f$  also. By virtue of this definition, the total heat transfer  $Q_T$  in a finned tube of length  $L$  carrying a high temperature gas flow may be easily obtained from an overall energy balance between any two consecutive stations  $z = 0$  (the entrance) and  $L$  (any downstream station), i.e.

$$Q_T = \dot{m}c_p(T_{\text{bL}} - T_c). \quad (10)$$

Likewise, upon introduction of an ideal heat transfer  $Q_x$  between  $z = 0$  (the entrance) and  $\infty$  (an axial station placed far away from the entrance)

$$Q_x = \dot{m}c_p(T_w - T_c) \quad (11)$$

the bulk temperature ratio  $T_{\text{bL}}/T_{\text{ref}}$  may be associated with the heat transfer efficiency  $\Omega$ . In ratio form, this efficiency simply becomes

$$\Omega = \frac{Q_T}{Q_x}. \quad (12)$$

Consequently, combining equations (10)–(12) yields the efficiency–temperature relation

$$\Omega = \frac{t_c - t_{\text{bL}}}{t_c - 1} \quad (13)$$

which in essence serves to associate the dimensionless mean bulk temperature  $t_{\text{bL}}$  (at a certain station  $z = L$ ) with the total heat transferred up to that station in the finned tube,  $Q_T$ .

To visualize the enhancement effect caused by internal finning, the inside tube diameter, rather than the equivalent hydraulic diameter, is used as the characteristic dimension in the axial coordinate  $Z^+$ . Accordingly, this dimensionless quantity  $Z^+$  computed by the relation

$$\frac{Re}{Re_s} = \frac{Z^+}{Z} \quad (14)$$

is adopted here for presenting the set of hydrodynamic and thermal results.

### COMPUTATIONAL PROCEDURE

The computational task consists of the solution of equations (1)–(6), which eventually will provide the velocity, temperature and heat flux fields in the convective–radiative medium. Accordingly, the system of partial differential equations was solved numerically by the control volume procedure described by Patankar [17], in conjunction with the SIMPLER code [18].

Alternatively, for the contribution of the radiatively participating gas, the two-dimensional RTE is modeled by an approximate differential method. In this work, the first-order spherical harmonics ( $P_1$ -approximation) has been employed. It supplies an additional elliptic equation of diffusion–convection type, namely equation (A11), which is derived in the Appendix. Thus, the discretization introduced to obtain a finite-difference form of the RTE employs the same control volumes utilized for the conservation equations of momentum and energy. Correspondingly, the special feature of this formulation/computational approach is that the full set of conservation equations are of the general diffusion–convection form, namely

$$\frac{\partial}{\partial x_j} \left( \rho U_j \phi - \Gamma_\phi \frac{\partial \phi}{\partial x_j} \right) = S_\phi \quad (15)$$

which is fully compatible with the SIMPLER code. The terms  $\Gamma_\phi$  and  $S_\phi$  in equation (15) are the diffusion coefficient and source term, respectively.

Once the control volume discretization is com-

Table 1. Comparison of the friction factor,  $f Re$ 

$H$	$NF = 4$		$NF = 8$		$NF = 16$	
	(1)	(2)	(1)	(2)	(1)	(2)
0.5	41.89	40.84	89.15	82.54	182.96	169.26
0.8	80.11	82.54	221.88	215.44	877.53	868.70

(1) Present work.

(2) Soliman and Feingold [16].

pleted, the procedure for solving the corresponding set of algebraic equations relies on the common practice of solving them by a standard line-by-line method [17]. This method involves solving simultaneously for all the variables along one grid line, which of course may be accomplished by an efficient algorithm. In this context, the line-by-line scheme was supplemented by a standard block-correction procedure which employs the concept of additive corrections generalized by Settari and Aziz [19]. Furthermore, at this stage it should be emphasized that since the energy and radiative transfer equations are interlinked, both were solved iteratively at each axial station  $Z$  in the thermal entrance region.

The computations were performed with uniform spacings on a  $22 \times 22$  grid in the  $\eta-\theta$  coordinates utilized here. In addition, a non-uniform axial step was used for the thermal calculations starting from a small value of  $Z = 10^{-5}$  at the entrance, and subsequently adjusted gradually in the downstream region of the tube. With regards to the grid size, preliminary runs on grids that were finer indicated that the results presented are accurate to at least 1% in the primitive and overall variables at a station close to the entrance  $Z = 10^{-4}$ . As expected, the accuracy improves significantly at stations further downstream in the tube. As a verification of the computational procedure, numerical results were obtained initially for a conventional fluid flow through finned tubes without participating radiation. For these tubes, numerical values of the friction factor represented by  $f Re$  were compared in Table 1 with the analytical predictions reported by Soliman and Feingold [16]. In general, these comparisons for  $\beta = 3^\circ$  resulted in good agreement for all tube geometries tested. Additional results were determined later for high temperature gas flows ( $Pr = 0.7$ ) through finless tubes accounting for participating radiation. Correspondingly, for the situation involving combined forced convection and radiation in a plain tube, the mean bulk temperature distribution based on the  $P_1$ -approximation agrees well with the classical solutions of Pearce and Emery [8] and Echigo *et al.* [9] for a wide range of radiation parameters considered. To conserve space, these comparisons are not included in this paper, but they are discussed in detail in ref. [11].

On the other hand, for radiative transfer in axisymmetric, finite cylindrical enclosures Mengüç [20] compared the predictions based on the  $P_1$ - and  $P_3$ -approximations with the 'exact' numerical results.

He found that the maximum difference between the heat fluxes using the exact data and the  $P_N$ -results was at most 10%. According to ref. [20], the discrepancy was not expected to be critical when radiation is coupled with other modes of heat transfer.

In light of the foregoing discussion, the mathematical formulation of the problem under study here relies on the  $P_1$ -approximation. Additionally, the solution of equations (1)–(6) was carried out numerically using control volumes, the SIMPLER code and the mesh described in the preceding paragraphs.

## RESULTS AND DISCUSSION

An examination of the dimensionless set of conservation equations reveals the presence of six prescribable parameters: (1) the number of fins  $NF$ , (2) the fin angle  $2\beta$ , (3) the dimensionless fin height  $H$ , (4) the entrance-to-wall temperature ratio  $t_e$ , (5) the optical thickness  $\tau$  and (6) the radiation-conduction parameter  $N$ . In order to minimize the number of figures in the presentation of results the calculations correspond to  $\beta = 3^\circ$ ,  $H = 0.5$  and  $t_e = 0.5$ , respectively. In light of this, the numerical computations were carried out for three different fin arrangements:  $NF = 0, 3$  and  $5$ . The radiation parameters considered were  $\tau$  and  $N$ , their numerical values ranging as  $0 < \tau < 5$  and  $0 < N < 10$ , respectively. This choice of parameters covers a spectrum of possible combinations of high temperature gas flows under laminar motion.

The development of the temperature profiles along the length of the longitudinal finned tubes may be conveniently studied by means of the axial variation of the mean bulk temperature  $t_b$ . In fact, as stated earlier, the bulk temperature at any axial location is a better indication of the thermal development than the Nusselt number because by virtue of equation (13) it also represents the total heat removal  $Q_T$  from the gas flow until that axial location. Although the Nusselt number is traditionally the dimensionless parameter employed in presenting results for internal forced convection problems, there is a good justification not to adopt this approach here. For engineering purposes, the most important information is the heat transfer enhancement in a certain tube length due to the addition of fins with respect to a similar finless tube. Correspondingly, this objective may be accomplished by combining the mean bulk temperature distribution and equation (13).

For a standard case of forced convection in a finned tube without participating radiation, Fig. 2 shows the development of  $t_b$  over the region  $10^{-3} < Z^+ < 1$  for  $NF = 0, 3$  and  $5$ , respectively. The mean bulk temperature development for any Prandtl number fluid (either gas or non-metallic liquid) starts with  $t_b = 0.5$  for a different number of fins in the array. As  $NF$  increases from 0 to 5,  $t_b$  follows the expected behavior of monotonic increase along the developing region down to the asymptotic region, wherein thermal satu-

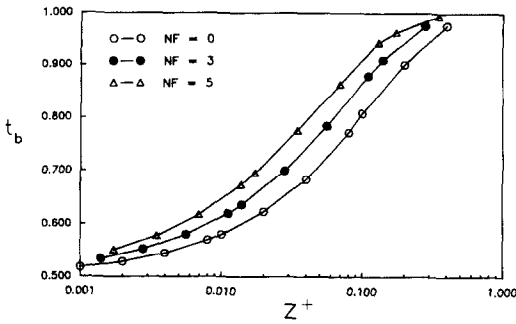


FIG. 2. Mean bulk temperature distribution for  $\tau = 0$  and  $N = 0$ .

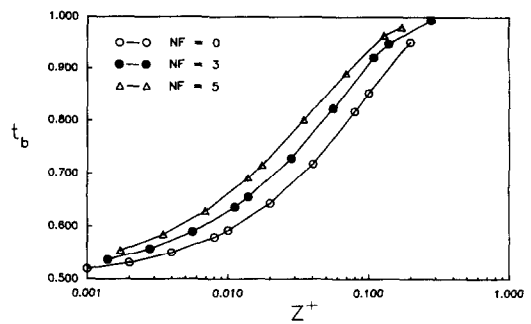


FIG. 6. Mean bulk temperature distribution for  $\tau = 0.05$  and  $N = 5$ .

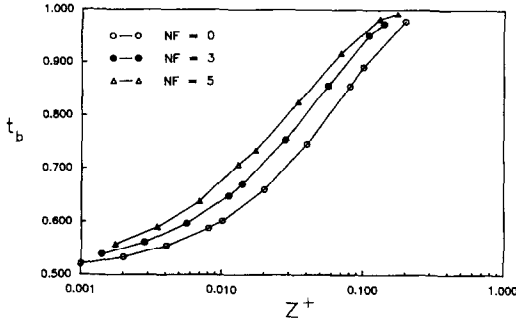


FIG. 3. Mean bulk temperature distribution for  $\tau = 1$  and  $N = 1$ .

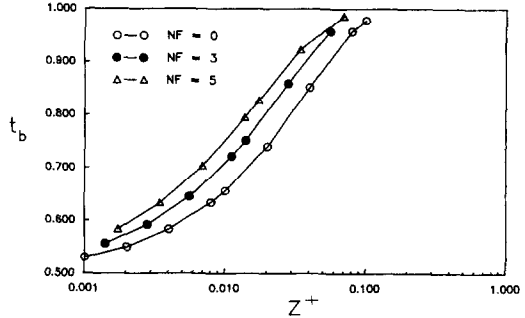


FIG. 7. Mean bulk temperature distribution for  $\tau = 5$  and  $N = 5$ .

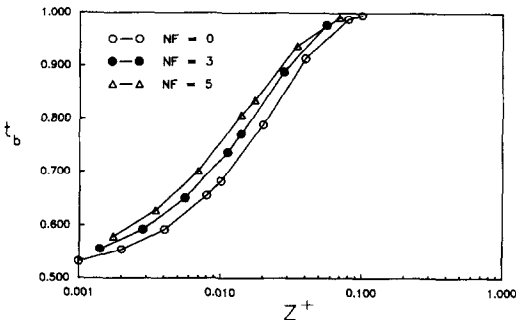


FIG. 4. Mean bulk temperature distribution for  $\tau = 1$  and  $N = 5$ .

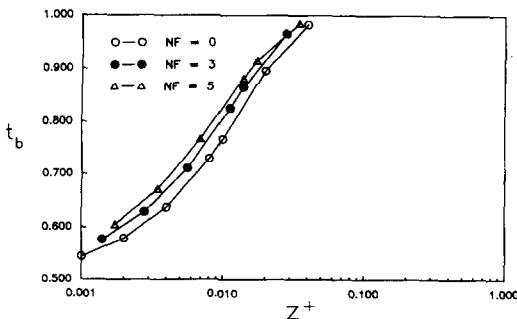


FIG. 5. Mean bulk temperature distribution for  $\tau = 1$  and  $N = 10$ .

ration occurs. In this figure, all finned tubes appear to have approximately the same axial temperature gradient in a large portion of the thermal entrance region.

Figures 3–7 have been prepared to show the influence of participating thermal radiation in a gas flow

( $Pr = 0.7$ ) through a finned tube, being represented by various values of the optical thickness  $\tau$  and the radiation-conduction parameter  $N$ . At this juncture, note should be taken that although  $Pr = 0.7$ , the flow rate described by the Reynolds number  $Re$  appears as an indirect parameter in the dimensionless axial distance  $Z^+$ .

The major issue to be examined in Figs. 3–5 is the response of the mean bulk temperature development to changes in  $N$  maintaining a fixed value of  $\tau$ , for instance  $\tau = 1$ . First, considering Fig. 3 where  $N = 1$  it is seen that the bulk temperatures increase rather slowly with  $Z^+$  and that the difference between the curves remains approximately unaltered. As expected, the region of thermal saturation for each curve occurs at a shorter value of  $Z^+$  when compared with the situation without radiation (see Fig. 2). This behavior is due to the relatively low rates of radiative transfer taking place in the gas.

Conversely, when radiation is stronger  $N = 5$ , the afore-mentioned trends are modified as evidenced in Fig. 4. Accordingly, the mean bulk temperature for each group of fins rises more rapidly than before. Furthermore, the effect of the number of fins is heightened, especially for  $NF = 3$  and 5. Here, it is also seen that with the addition of fins, the deviations of local bulk temperature  $\Delta t_b$  at each station tend to decrease as the number of fins increase from 0 to 3, and finally to 5. Correspondingly, the gas flow reaches the wall temperature at  $Z^+ = 0.10$ . The presentation of results for  $\tau = 1$  is completed in Fig. 5. Here, temperature results show a pronounced sensitivity to radiation as  $N$  increases to 10. For this situation, heat transfer rates increase in the thermal entrance region causing

Table 2. Mean bulk temperature at  $Z^+ = 0.01$  for  $N = 5$ 

NF	$\tau$		
	0.05	1	5
0	0.590	0.777	0.650
3	0.625	0.816	0.709
5	0.654	0.836	0.755

Table 3. Mean bulk temperature  $Z^+ = 0.05$  for  $N = 5$ 

NF	$\tau$		
	0.05	1	5
0	0.766	1	0.893
3	0.818	1	0.950
5	0.855	1	0.964

more rapid changes in  $t_b$ . The trends in this figure are in agreement with those discussed in the foregoing paragraphs for Fig. 4, but certain details are worth noting. It is evident that as  $NF$  surpassed 5, the mean bulk temperature variation is moderately sensitive to the number of fins utilized in the array. For this particular case, the gas flow reaches the asymptotic thermal condition at  $Z^+ = 0.04$  and conversely, the pressure gradient is appreciably augmented. The foregoing behavior may be summarized as follows. As  $N$  increases, the numerical results tend to approach an asymptotic solution which is independent of  $N$ . This solution seems to be invariant with the addition of more fins. In fact, letting  $N \rightarrow \infty$  in equation (2) gives  $G^* = t^4 = 0$ . This relation yields  $G^* = \text{constant}$  from the combination of equations (3)–(5). Therefore,  $t = G^{*1/4} = \text{constant}$  indicates that the result is indeed independent of geometry.

Results for variable  $\tau$  comprise the final item in the presentation of results specifically for values of  $\tau = 0.05, 1, 5$  retaining  $N = 5$ . The main feature of the results illustrated in Fig. 6 for  $\tau = 0.05$  and  $N = 5$  is the evidence of low rates of heat transfer. The mean bulk temperatures do not differ much from those of Fig. 3 for  $\tau = 1$  and  $N = 1$ , wherein the parameters appear to have a compensatory effect.

The discussion of Figs. 6, 4 and 7 will be done with the help of the numerical results of Tables 2 and 3. From a detailed inspection of these figures, it appears that the response of  $t_b$  to  $\tau$  is analogous to the response of  $t_b$  to  $N$  discussed previously. Attention is first focused on a finned tube having a fixed dimensionless length of  $Z^+ = 0.01$ . An examination of Table 2 reveals a rather interesting thermal behavior. The maximum value of  $t_b$  (or its equivalent the maximum heat removal  $Q_{T\text{max}}$ ) occurs in the vicinity of  $\tau = 1$ , regardless of the number of fins in the bundle. This phenomenon is an indication of the sweeping effect that  $\tau$  possesses on the gas temperature, reaching maximum values at approximately  $\tau = 1$ , and thereafter dropping slightly depending on the number of fins considered. To complete this discussion, attention

is now turned to a larger finned tube with a constant dimensionless length of  $Z^+ = 0.05$ . For this case, the corresponding mean bulk temperature results are tabulated in Table 3, and here again, approximate maximum values of  $t_b$  are associated to  $\tau = 1$  for any number of fins in the array. In passing, it should be mentioned that the influence of the optical thickness  $\tau$  ( $\tau = 1$ ) on the maximum heat transfer has been also observed in ref. [11] for the situation of plain tubes.

## CONCLUSIONS

The enhancing effects of longitudinal fins have been studied for cases of forced convection with participating radiation in laminar gas tube flow. Under the assumption of a gray gas, the two-dimensional radiative transfer equation has been modeled by the  $P_1$ -approximation. The methodology proposed here appears to circumvent several of the computational difficulties encountered in convective–radiative problems. A detailed inspection of the numerical results leads to the conclusion that large errors will arise in the analysis when radiation is neglected for high temperature gas flows. The conclusions may be recast as follows: as the radiation–conduction parameter  $N$  increases, the numerical results approach an asymptotic solution, which seems to be invariant with the addition of more fins. On the contrary, the influence of the optical gas thickness  $\tau$  is more complicated, because maximum heat removal is achieved whenever  $\tau = 1$  approximately. Ultimately, the enhancing factor due to the inclusion of the radiative mechanism is explained in detail.

*Acknowledgements*—The authors wish to express their appreciation to one of the reviewers for providing constructive comments during the review process of the manuscript.

## REFERENCES

1. A. E. Bergles, Some perspective on enhanced heat transfer: second generation heat transfer technology, *J. Heat Transfer* **110**, 1082–1096 (1988).
2. I. M. Rustom and H. M. Soliman, Numerical analysis of laminar forced convection in the entrance region of tubes with longitudinal internal fins, *J. Heat Transfer* **110**, 310–313 (1988).
3. C. Prakash and Y. D. Liu, Analysis of laminar flow and heat transfer in the entrance region of an internally finned circular duct, *J. Heat Transfer* **107**, 84–91 (1985).
4. D. Choudhary and S. V. Patankar, Analysis of developing laminar flow and heat transfer in tubes with radial internal fins, *Proc. ASME Natn. Heat Transfer Conf.*, pp. 57–63 (1985).
5. J. R. Howell, Thermal radiation in participating media: the past, the present and some possible futures, *J. Heat Transfer* **110**, 1220–1229 (1988).
6. Y. Mori, A. E. Sheindlin and N. H. Afgan, *High Temperature Heat Exchangers*. Hemisphere, New York (1986).
7. B. E. Pearce, Heat transfer by thermal radiation and forced convection in an absorbing fluid in the entrance region of a tube, Ph.D. Thesis, University of Washington, Seattle, Washington (1968).
8. B. Pearce and A. Emery, Heat transfer by thermal radiation and laminar forced convection to an absorbing

fluid in the entry region of a pipe, *J. Heat Transfer* **92**, 221–230 (1970).

9. R. Echigo, S. Hasegawa and K. Kiramuto, Composite heat transfer in a pipe with thermal radiation of two-dimensional propagation in connection with the temperature rise in a flowing medium upstream of a heating section, *Int. J. Heat Mass Transfer* **18**, 1149–1159 (1975).
10. N. Ozisik, *Radiative Transfer*. Wiley, New York (1973).
11. A. Campo and C. Schuler, Thermal radiation and laminar forced convection in a gas pipe flow, *Wärme- und Stoffübertr.* **22**, 251–257 (1988).
12. Y. Kurosaki, Heat transfer by radiation and other transport mechanisms, *Bull. Jap. Soc. Mech. Engrs* **14**, 572–580 (1971).
13. T. Chawla and S. H. Chan, Combined radiation-convection in thermally developing Poiseuille flow, *J. Heat Transfer* **102**, 297–302 (1980).
14. K. Torikoshi, M. Kawazoe, M. Fujiwara and Y. Kurosaki, Heat transfer augmentation due to surface radiative exchange in internal fins in an annulus, *Proc. ASME Natn. Heat Transfer Conf.*, HTD 72, pp. 91–97 (1987).
15. S. H. Chan and K. Kumar, Analytical investigation of SER recuperator performance, *Proc. Energy-sources Technol. Conf. Exhibition*, PD 30, pp. 161–168 (1989).
16. H. M. Soliman and A. Feingold, Analysis of fully developed laminar flow in longitudinal finned tubes, *Chem. Engng J.* **14**, 119–128 (1977).
17. S. V. Patankar, *Numerical Heat Transfer and Fluid Flow*. Hemisphere, New York (1980).
18. S. V. Patankar, A general-purpose computer program for two-dimensional elliptic situations, Department of Mechanical Engineering, University of Minnesota (1982).
19. A. Settari and K. Aziz, A generalization of the additive correction methods for the iterative solution of matrix equations, *SIAM J. Numer. Analysis* **10**, 506–521 (1973).
20. M. P. Mengüç, Modeling of radiative heat transfer in multidimensional enclosures using spherical harmonics approximation, Ph.D. Thesis, Purdue University (1985).
21. H. Schlichting, *Boundary Layer Theory*. McGraw-Hill, New York (1979).
22. D. K. Hennecke, Heat transfer by Hagen-Poiseuille flow in the thermal development region with axial conduction, *Wärme- und Stoffübertr.* **1**, 177–183 (1968).

## APPENDIX. MODELING OF RADIATIVE TRANSFER IN THE MEDIUM

The radiative heat flux vector  $\mathbf{q}^R$  may be expressed in terms of the intensity of radiation as follows [10]:

$$\operatorname{div}(\mathbf{q}^R) = \int_{4\pi} K_a [I_b(T) - I(\boldsymbol{\Omega}, s)] d\omega \quad (\text{A1})$$

where the first and second terms of the integrand represent the emitted and absorbed radiation in the participating medium, respectively. Additionally, the intensity of radiation may be written as

$$I(\mathbf{p}, \boldsymbol{\Omega}) = I_0(\mathbf{p}) + a(\mathbf{p}) \cdot l + b(\mathbf{p}) \cdot m + c(\mathbf{p}) \cdot n \quad (\text{A2})$$

where  $a$ ,  $b$ ,  $c$  are functions of position and  $l$ ,  $m$ ,  $n$  are the direction cosines in the  $\boldsymbol{\Omega}$ -direction.

### $P_1$ -approximation

Upon integrating the RTE in cylindrical coordinates yields a partial differential equation for the first moment of intensity  $I_0$

$$\frac{\partial^2 I_0}{\partial z^2} + \frac{1}{r} \frac{\partial}{\partial r} \left( r \frac{\partial I_0}{\partial r} \right) + \frac{1}{r^2} \frac{\partial^2 I_0}{\partial \theta^2} = 3\beta K_a (I_0 - I_b) \quad (\text{A3})$$

where  $\beta$  is the extinction coefficient of the participating medium.

Alternatively, combining equations (A1) and (A2) and

carrying out the required integration steps, results in the relation between the radiative heat flux and the intensity of radiation, i.e.

$$\operatorname{div}(\mathbf{q}^R) = 4\pi K_a (I_b - I_0). \quad (\text{A4})$$

Furthermore, the definition of the total irradiation  $G$

$$G = \int_{4\pi} I d\omega \quad (\text{A5})$$

when combined with equation (A2) leads to the relation

$$G = 4\pi I_0. \quad (\text{A6})$$

In addition, owing to the hypothesis of local thermodynamic equilibrium, the intensity of radiation for a black body  $I_b$  becomes

$$I_b = \sigma T^4/\pi. \quad (\text{A7})$$

By virtue of the previous definitions, the equation of energy conservation [21] and the equation of radiative transfer, equation (A3), may be transformed into the following system of partial differential equations:

$$u(r) \frac{\partial T}{\partial z} = \frac{k}{\rho c_p} \left[ \frac{1}{r} \frac{\partial}{\partial r} \left( r \frac{\partial T}{\partial r} \right) + \frac{1}{r^2} \frac{\partial^2 T}{\partial \theta^2} \right] + \frac{K_a}{\rho c_p} (G - 4\sigma T^4) \quad (\text{A8})$$

$$\frac{\partial^2 G}{\partial z^2} + \frac{1}{r} \frac{\partial}{\partial r} \left( r \frac{\partial G}{\partial r} \right) + \frac{1}{r^2} \frac{\partial^2 G}{\partial \theta^2} = 3\beta K_a (G - 4\sigma T^4) \quad (\text{A9})$$

where the dependent variables are the temperature  $T$  and the irradiation  $G$ . Under the assumption of a non-scattering gray medium and introducing the dimensionless quantities defined in equation (6), leads to a new system controlling the temperature and heat flux fields. That is

$$U/(2\bar{U}) \frac{\partial t}{\partial Z} = \frac{1}{\eta} \frac{\partial}{\partial \eta} \left( \eta \frac{\partial t}{\partial \eta} \right) + \frac{1}{\eta^2} \frac{\partial^2 t}{\partial \theta^2} + 4N\tau(G^* - t^4) \quad (\text{A10})$$

$$\frac{1}{(Re Pr)^2} \frac{\partial^2 G^*}{\partial Z^2} + \frac{1}{\eta} \frac{\partial}{\partial \eta} \left( \eta \frac{\partial G^*}{\partial \eta} \right) + \frac{1}{\eta^2} \frac{\partial^2 G^*}{\partial \theta^2} = 3\tau^2(G^* - t^4). \quad (\text{A11})$$

A detailed inspection of these equations reveals that equation (A10) is a three-dimensional equation of the parabolic type, whereas equation (A11) is a three-dimensional equation of the elliptic type.

Next, in order to obtain an a priori estimate of the conditions for which the axial transport of thermal radiation in the tube can be neglected, an order of magnitude argument similar to that used in the boundary layer theory [21] has been made. In fact, such an argument was developed by Pearce [7] for laminar forced convection with a radiatively participating gas through circular plain tubes. His reasoning was based on the observation that the radiation flux in the optically thick limit will yield the most conservative criterion for purposes of analysis. Here, this requirement may be written as follows:

$$\rho c_p \bar{u} \frac{\partial T}{\partial z} \gg \frac{\partial q_z^R}{\partial z}. \quad (\text{A12})$$

Thus, this inequality is indeed a statement that the contribution of the axial component of the radiation heat flux is very much smaller than that of the equivalent axial convection term. Consequently, in the optically thick limit (an upper bound), the radiation heat flux is simply given by

$$q_z^R = \frac{16\sigma T_{\text{ref}}^3}{3K_a} \frac{\partial T}{\partial z}. \quad (\text{A13})$$

This criterion, when written in the context of the present problem, simply becomes



$$\frac{3\bar{\rho}\bar{u}c_p K_a r_o}{16\sigma T_{\text{ref}}^3} \gg 1. \quad (\text{A14})$$

Equivalently, the radiation Peclet number defined as  $Pe_R = Re Pr(\tau/N)$  is restricted by the inequality

$$Re Pr(\tau/N) \gg 10 \quad (\text{A15})$$

which dictates the criterion for neglecting axial thermal radiation in equation (A11). In this sense, condition (A15) is analogous to  $Re Pr \gg 1$  which according to Hennecke [22] provides the threshold of axial heat conduction in purely forced convection tube flows.

In light of the foregoing order-of-magnitude analysis, equation (A11) in the absence of axial thermal radiation, becomes

$$\frac{1}{\eta} \frac{\partial}{\partial \eta} \left( \eta \frac{\partial G^*}{\partial \eta} \right) + \frac{1}{\eta^2} \frac{\partial^2 G^*}{\partial \theta^2} = 3\tau^2(G^* - t^4). \quad (\text{A16})$$

Hence, from a computational point of view, this simplification is extremely advantageous because equation (A11) becomes a two-dimensional equation retaining its elliptic structure in the cross-stream direction only, and not in the axial direction.

#### *P<sub>3</sub>-approximation*

For the  $P_3$ -approximation, after some elaborate manipulations of the moment-differential equations four elliptic partial differential equations are obtained. These four equations where the dependent variables are the  $l_0$ ,  $l_{11}$ ,  $l_{33}$  and  $l_{13}$  moments have to be solved simultaneously. Consequently, an iterative scheme must be employed to obtain the solution of the four moments of the intensity of radiation. Once the magnitude of the intensity is known, the radiative flux distribution may be written.

### AMELIORATION DU TRANSFERT THERMIQUE DANS LES TUBES AILETES INTERIEUREMENT EN TENANT COMPTE DE LA COMBINAISON DE LA CONVECTION ET DU RAYONNEMENT

**Résumé**—On présente une analyse du transfert thermique simultané par convection forcée, rayonnement et conduction dans la région d'entrée d'un tube circulaire aileté intérieurement. Les équations de quantité de mouvement, d'énergie et de transfert radiatif sont résolues numériquement en utilisant une méthode de volume de contrôle. Dans l'idéalisation de gaz gris, la contribution du rayonnement dans le milieu est modélisé par une méthode différentielle approchée, l'approximation harmonique sphérique du premier ordre ( $P_1$ ). Cette approche fournit une équation additionnelle aux dérivées partielles du type elliptique dans le système d'équations de convection. L'adoption de cette formulation différentielle est avantageuse du point de vue numérique, parce qu'elle est compatible avec le code SIMPLER. Les résultats du calcul pour les profils de vitesse distordus dans la section droite réduite du tube donnent les pertes par frottement dues à l'addition des ailettes longitudinales. L'augmentation du transfert thermique dans l'entrée thermique du tube aileté est représentée par la température moyenne du fluide en fonction des paramètres descriptifs qui sont géométriques, hydrodynamiques, thermiques et radiatifs.

### ERHÖHUNG DES WÄRMEÜBERGANGS IN INNENBERIPPTE ROHREN UNTER BERÜCKSICHTIGUNG VON KONVEKTION UND STRAHLUNG

**Zusammenfassung**—In dieser Arbeit wird der gekoppelte Wärmetransport durch erzwungene Konvektion, Strahlung und Leitung im Einlaufbereich eines innenberippten kreisförmigen Rohres analysiert. Die Erhaltungsgleichungen für Impuls, Energie und Strahlungstransport werden mit Hilfe eines Kontrollvolumenansatzes numerisch gelöst. Bei einer Idealisierung als graues Gas wird der Strahlungsanteil mit einer Differenzmethode, die auf einer sphärischen harmonischen Näherung erster Ordnung beruht, berechnet. Dadurch ergibt sich eine zusätzliche elliptische Differentialgleichung im System der Differentialgleichungen. Diese Vorgehensweise bringt Vorteile bei der Simulation mit sich, da sich eine vollständige Kompatibilität mit dem SIMPLER-Code ergibt. Berechnungen des verzerrten Geschwindigkeitsprofils im verengten Rohrquerschnitt liefern die zusätzlichen Reibungsverluste aufgrund der Längsrippen. Außerdem wird die Erhöhung des Wärmeübergangskoeffizienten im thermischen Einlaufgebiet (bezogen auf die mittleren Temperaturen) in Abhängigkeit von den entscheidenden geometrischen, hydrodynamischen, thermischen und optischen Parametern dargestellt.

### ИНТЕНСИФИКАЦИЯ ТЕПЛОПЕРЕНОСА В ТРУБАХ С ВНУТРЕННИМ ОРЕБРЕНИЕМ С УЧЕТОМ СМЕШАННОЙ КОНВЕКЦИИ ПРИ НАЛИЧИИ РАДИАЦИИ

**Аннотация**—Анализируется совместный теплоперенос за счет вынужденной конвекции, радиации и теплопроводности во входном участке круглой трубы с внутренним оребрением. С использованием метода, основанного на контрольном объеме, численно решаются уравнения импульса, энергии и радиационного переноса. В приближении серого газа вклад излучения в среде моделируется с помощью дифференциального метода и с использованием приближения сферических гармоник первого порядка ( $P_1$ ). Предложенный подход позволяет получить дифференциальное уравнение эллиптического типа, дополняющее в систему уравнений конвекции-диффузии. Использование указанной дифференциальной формулировки удобно с точки зрения вычислений. Результаты, полученные для деформированных профилей скоростей в уменьшенном поперечном сечении трубы, позволяют определять потери на трение, вызванные наличием продольного оребрения. Кроме того, интенсификация теплопереноса во входном тепловом участке оребренной трубы представлена средней объемной температурой через наглядные геометрические, гидродинамические, тепловые и радиационные параметры.